JOURNAL OF CATALYSIS **131**, 60–73 (1991)

The Interaction of Hydrocarbons with Copper–Nickel and Nickel in the Formation of Carbon Filaments

M. S. KIM, N. M. RODRIGUEZ, AND R. T. K. BAKER

Chemical Engineering Department, Auburn University, Auburn, Alabama 36849

Received September 17, 1990; revised March 5, 1991

We have carried out a comprehensive investigation of the interaction of selected hydrocarbons with copper–nickel and nickel catalysts. Detailed analysis of both the yield of gaseous products and the amount of solid carbon deposited on the catalyst surfaces has enabled us to account for the entire course of the reaction and postulate the structural arrangements of reactive intermediates formed in the various systems. The excessive amount of methane produced from the copper–nickel/ethylene interaction cannot be accounted for purely on the basis of hydrogasification and is believed to result from the formation of an "ethylidyne" intermediate. In contrast, nickel forms a strong bond with both carbon atoms in the hydrocarbon and in this case only minor amounts of methane are produced. It was found that copper–nickel reacted very readily with ethylene at 600°C, whereas under the same conditions the presence of hydrogen was required to moderate interaction between the hydrocarbon and nickel. Both catalysts underwent direct reaction with acetylene at 600°C, but showed no tendency to decompose methane at temperatures below 900°C.

INTRODUCTION

The interaction of hydrocarbons with metal surfaces can result in a variety of reactions, one of which is the formation of filamentous carbon. This type of material is formed exclusively in systems where a catalyst is present and is believed to involve the interaction and subsequent decomposition of the hydrocarbon at particular faces of the metal. *In situ* electron microscopy studies (*1*) have not only shown the qualitative features by which the catalyst operates in the formation of filamentous carbon, but also have provided the kinetic data which led to the postulation of a growth mechanism. Following hydrocarbon decomposition, carbon species diffuse through the catalyst particle and eventually precipitate at the rear surfaces to form the filament structure. The postulate that carbon diffusion through the catalyst particle is the rate-determining step is supported by the agreement between the measurements of activation energies for filament growth with those for carbon diffusion through the respective metals. In general, filaments produced from single-metal catalysts tend to adopt a whisker-like form where the catalyst particle is carried away from the support during the growth process and remains at the tip of the filament. It is believed that growth ceases when the leading face of the catalyst is encapsulated by a layer of carbon built up as a consequence of overall rate control by the carbon diffusion process. This condition can also occur as the result of a change in the adsorption properties of the particle brought about by crystallographic rearrangements.

Transition metals such as iron, cobalt, and nickel are known to be very active catalysts for carbon filament formation (*1–4*), whereas other metals including copper absorb hydrocarbons but do not appear to break carbon–carbon bonds and as a consequence do not catalyze the growth of this form of carbon (*4*). The recent trend in these studies has been to examine the manner by which additives to the catalyst particle modify the filament growth characteristics and in this context, addition of copper to nickel has been reported to significantly change the

0021-9517/91 $3.00

rate of reaction leading to carbon deposition (*5–9*).

Copper–nickel is one of the most widely studied bimetallic systems in the field of heterogeneous catalysis. Copper appears to be relatively inactive for most reactions unless it is combined with a promoter. Although the mechanism by which nickel enhances the catalytic activity of copper remains unclear, the behavioral patterns exhibited by the bimetallic system in various catalytic reactions have been extensively investigated (*10–20*). Early catalytic studies on copper–nickel alloys were inspired by the work of Dowden and Reynolds (*21, 22*). Since the heat of sublimation of copper is lower than that of nickel, it is expected that copper atoms will tend to segregate to the surface of bimetallic particles. This behavior has been observed experimentally under reducing conditions (*15, 23, 24*). The reduction in the size of ensembles of nickel atoms brought about by the presence of copper has been demonstrated by Ponec to be directly related to the changes in catalytic activity (*25, 26*).

Comprehensive reviews of the behavior of bimetallic catalysts (*27, 28*) have dealt with the question of how the catalytic activity and selectivity of a metal is modified by alloying and two effects have been considered: (a) the electronic structure effect, where the properties of a component in the alloy surface are different from those of the pure metal, and (b) the geometric effect, where ensembles of more than one atom of a particular component are less frequently encountered in the surface of an alloy than in the pure metal.

The majority of studies dealing with carbon deposition on metals have tended to focus on the identification of the type of solid carbon formed in these reactions and little emphasis has been placed on the consideration of the manner by which the hydrocarbons bond and ultimately react with the metal surface. This aspect, however, has been extensively investigated by surface science techniques on single-crystal surfaces under somewhat idealized conditions of temperature and pressure (*29, 30*).

In the current investigation, we have endeavored to take a broader view of the interaction of hydrocarbons with metal surfaces by taking into account all the products of the reaction. In this regard, carbon deposition, hydrogasification, and decomposition of selected hydrocarbons over copper–nickel and nickel are used as probe reactions in order to gain a clearer understanding of the steps involved in these systems. A careful determination of the amount of carbon deposit coupled with an analysis of the gaseous products has been used in conjunction with the data available from surface science studies to reconstruct the steps involved in the reaction between the metal surface and the adsorbed hydrocarbons and predict the reactive intermediates which are formed in the processes.

EXPERIMENTAL

Materials

The copper–nickel powder catalysts used in these studies were prepared by coprecipitation of the metal carbonates from mixed nitrate solutions using ammonium bicarbonate. The detailed procedure is well described by Sinfelt *et al.* (*15*) and Best and Russell (*10*). The precipitate was dried overnight at 110°C, and then calcined in air for 4 h at 400°C to convert the carbonate to mixed oxides, which were then reduced in hydrogen at 500°C in a quartz tube for 20 h to form the copper–nickel catalysts. The composition of the bimetallic powders was checked using energy dispersive X-ray spectroscopy (EDS). Nickel powders were prepared using a similar procedure. BET surface area measurements were carried out using nitrogen adsorption at −196°C. Values of $1.0 \pm 0.1\ \mathrm{m^2 \cdot g^{-1}}$ were obtained for both the bimetallic and nickel powders.

The gases used in this work, hydrogen (99.999%), acetylene (99.6%), ethylene (99.99%), methane (99.99%), helium (99.99%), and argon (99.99%) were obtained from Alphagaz Co. and were used without further purification. Reagent grade nickel nitrate [$Ni(NO_3)_2$ $6H_2O$] and Reagent grade cupric nitrate [$Cu(NO_3)_2$ $3H_2O$] were obtained from Fischer Scientific for the catalyst preparation.

Apparatus and Procedures

Carbon deposition experiments were performed in a quartz flow reactor (40 mm i.d. and 90 cm long) located in a Lindberg horizontal tube furnace. Flow rates of gases were controlled with needle valves and measured with rotameters. Catalyst samples (50–100 mg) contained in ceramic boats were reduced in a 10% hydrogen/helium stream for 2 h at the reaction temperature (usually at 600°C). Following this step a desired mixture of hydrocarbon, hydrogen, and inert gas was introduced into the reactor. The composition of the gas phase before and after the reaction was analyzed with a gas chromatograph (Varian 3400) using a 30-m megabore column (GS-Q). The column was temperature programmed to give hydrogen, methane, ethylene, acetylene, and ethane at 35°C and higher molecular weight hydrocarbons (C_3 to C_5) as the temperature was progressively raised to 180°C. The amount of carbon deposit produced on the catalyst after 1.5 h was determined by weight difference. In the current experimental arrangement, the formation of carbon filaments and gaseous product distributions were found to be independent of catalyst bed height since it was estimated that the overall conversion of the reactant hydrocarbon in the presence of an active catalyst was higher than 95%.

Rate measurements of both carbon deposition and carbon gasification were carried out in a Cahn 2000 microbalance reactor (vertical mullite tube, 48 mm i.d. and 60 cm long) fitted with a furnace. The furnace was attached to a controller and was capable of operating at temperatures up to 1100°C. The powdered catalyst (4 mg) was placed in a platinum pan hanging in the middle of the heated zone of the reactor where a constant temperature profile was maintained along its axis. Initially the reactor system was evacuated to remove residual air, and then filled with an inert gas such as argon or helium. The reactor was then brought to the operating temperature in a mixture of hydrogen and inert gas, and held at that temperature until the catalyst was completely reduced, usually 1 to 2 h. Carbon deposits were produced from a selected mixture of ethylene, hydrogen, and inert gas. A hydrogen/argon (1 : 1) mixture was used to gasify carbon deposits at various temperatures.

Transmission Electron Microscopy Examinations

The detailed structural characteristics of the deposited carbon were obtained from high-resolution transmission electron microscopy studies performed in a JEOL 200CX microscope. The specimens for these examinations were prepared by ultrasonic dispersion of a mass of the deposit in isobutanol and a drop of the suspension was applied to a carbon support film. The point to point resolution of the microscope is estimated to be 0.18 nm.

RESULTS

1. Characterization of Carbon Deposits

When the carbon deposits were examined by transmission electron microscopy they were found to consist almost entirely of filamentous carbon, with diamond-shaped catalyst particles located within the filament structures as presented in Fig. 1. The morphological characteristics of the filaments were identical for both nickel and copper–nickel catalysts. The filament widths were governed by the size of the associated catalyst particles and were typically in the range of 25 to 100 nm. It was significant that the active catalyst particles were considerably smaller than those of the original metal powders (estimated to be ~1 μm in diameter) which indicates that during the reaction

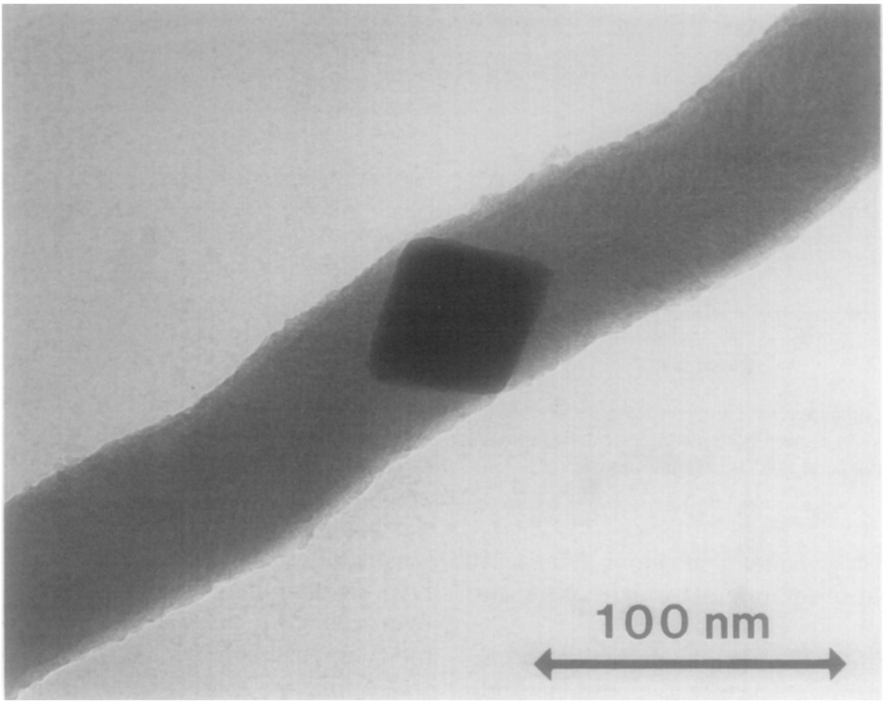

FIG. 1. Transmission electron micrograph showing the appearance of a carbon filament produced from the interaction of a copper–nickel catalyst particle with ethylene at 600°C.

fragmentation of the starting material occurred prior to carbon filament formation.

2. *Flow Reactor Studies*

2.1 Effect of copper–nickel ratio on carbon deposition. The influence of changing the ratio of copper to nickel on carbon deposition was studied in the flow reactor. These experiments were performed using pure ethylene at a flow rate of 40 ml/min at 600°C for 1.5 h over a constant weight of catalyst sample (50 mg). The weight of carbon produced during the reaction was determined and this value was used to compare the activity of the various catalyst samples.

As shown in Fig. 2, the weight of carbon was extremely sensitive to the catalyst composition. The amounts obtained on the mixed metal catalysts containing 30 to 80% nickel were relatively high. In contrast, nickel catalyst did not show any significant change in weight with pure ethylene. In this case a considerable amount of a tarry residue was observed at the outlet of the reactor indicating that polymerization reactions were favored.

2.2. Effect of reaction time on carbon deposition. In an attempt to learn more about the lifetime of catalyst particles during the formation of filamentous carbon, a series of experiments were conducted with various starting weights of copper–nickel (2:8) powders which were reacted for increasing time periods. The data obtained from these experiments is presented in Fig. 3, from which it can be seen that:

(i) The period of catalytic activity is dependent on the initial weight of the sample and provided sufficient material is present the carbon deposition rate remains constant for a relatively long time.

(ii) The weight of carbon deposit appears

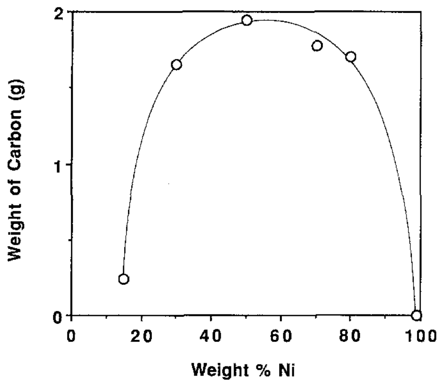

FIG. 2. Influence of catalyst composition on the weight of solid carbon produced from the decomposition of ethylene at 600°C (reaction time 1.5 h).

to reach a maximum of about 200 to 250 times that of the original weight of the catalyst.

2.3. Effect of inert gas additives on carbon deposition. The effect of inert gas additives to the hydrocarbon feed on the weight of carbon filaments produced is presented in Table 1. Reactions were carried out on the copper–nickel (3 : 7) catalyst at 600°C at a total flow rate of 100 ml/min. Inspection of these data shows that neither argon nor helium has any influence on the amount of hydrocarbon converted to carbon, even though the thermal conductivity of argon (9.3×10^{-5} cal/cm · s · deg) is significantly smaller than helium (84×10^{-5} cal/cm · s · deg) (*31*). Hence, it may be concluded that changes in the thermal conductivity of the gas environment do not play an important role in carbon deposition from the catalyzed decomposition of ethylene.

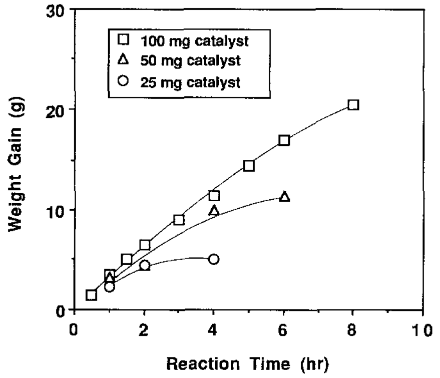

FIG. 3. Effect of time on the weight of solid carbon formed from the interaction of copper : nickel (2 : 8) catalysts with an ethylene–hydrogen (4 : 1) mixture at 600°C.

2.4. Effect of hydrogen on carbon deposition. The effect of adding increasing amounts of hydrogen to the ethylene feed on the formation of filamentous carbon on copper–nickel (3 : 7) and nickel catalysts is presented in Fig. 4. In the case of the bimetallic catalyst, the weight of carbon decreased in a monotonic fashion as the hydrogen content in the feed gas was increased. On the other hand with the pure nickel catalyst, the amount of carbon increased as the hydrogen content in the carrier gas was raised up to about 50% and then exhibited a steady decline with further adition of hydrogen.

To investigate further the differences between the bimetallic and pure nickel catalysts, two approaches were followed. First, measurement of the hydrogasification rates of the carbon deposit for the two catalyst systems was carried out in the presence of 360 Torr of hydrogen in the microbalance reactor facility. From the data presented in Fig. 5, it is clear that the bimetallic catalyst exhibits superior hydrogasification activity compared to that of pure nickel. For example, the gasification rate obtained with copper–nickel (3 : 7) was 100 times faster than that of pure nickel at 600°C.

In a complementary set of experiments, analysis of the gas composition at the exit of the flow reactor was performed after a period of 30 min, the minimum time for the yield of products to reach equilibrium. The results obtained with three different catalysts during reaction with an ethylene/hydrogen 4 : 1 mixture are presented in Fig. 6. In addition to unreacted ethylene and hydrogen other gases produced included methane, ethane, and trace amounts of C_3 and C_4 hy-

TABLE 1

Effect of Inert Gas Additives to the Hydrocarbon Feed on Carbon Deposition over Copper–Nickel (3 : 7) at 600°C

Additive	Ethylene: additive	Weight gain (g)	% Hydrocarbon conversion to carbon
None	100 : 0	5.91	74.4
Argon	80 : 20	5.14	72.8
	67 : 33	4.40	74.4
	50 : 50	3.25	73.6
	33 : 67	2.13	73.1
Helium	80 : 20	5.07	71.8
	67 : 33	4.48	75.7
	50 : 50	3.24	73.4
	33 : 67	2.09	71.7
	13 : 87	0.82	71.4
	10 : 90	0.66	74.7

drocarbons. Inspection of the data in Fig. 6 and Table 2 shows that for both copper–nickel catalysts methane is a major product. In contrast, methane formation was limited to about 1.0% of the reactant ethylene when pure nickel was used as the catalyst. When the hydrogen content of the reactant gas mixture was raised from 0 to 80 mole%, then from Table 2 it can be seen that the yield of ethane was found to exhibit a steady increase with both the bimetallic and pure nickel catalysts. However, based on the amount of ethylene converted in the reaction the yield of ethane is considerably higher for the latter system.

In order to ascertain the origin of the methane formed during the catalyzed carbon deposition process the following sequence of reactions was performed. Initially, the respective catalysts were treated in an ethylene/hydrogen 4 : 1 mixture at 600°C to produce carbon filaments and gas analysis carried out when the system reached equilibrium. Following this step, the reactant gas was removed by flushing the

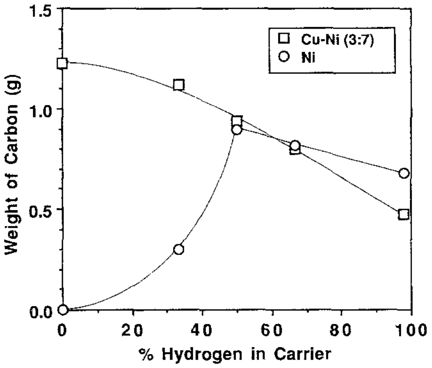

FIG. 4. Effect of hydrogen on the weight of solid carbon from the copper–nickel (3 : 7) and nickel-catalyzed decomposition of ethylene at 600°C (reaction time 1.5 h).

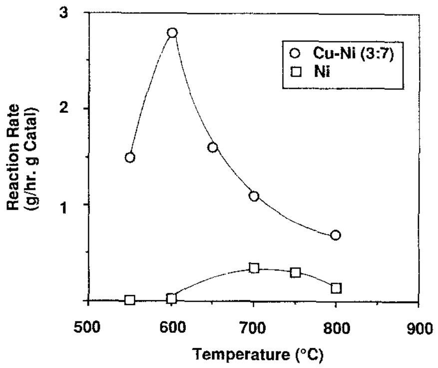

FIG. 5. Rate of hydrogasification of carbon in the presence of copper–nickel (3 : 7) and nickel as a function of temperature.

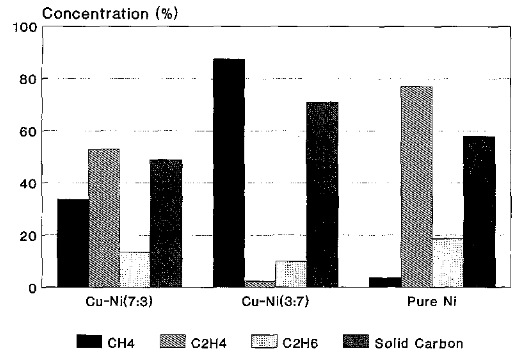

FIG. 6. Gaseous and solid carbon products from decomposition of an ethylene/hydrogen mixture (4 : 1) at 600°C as function of catalyst composition. (CH_4, C_2H_4, and C_2H_6 expressed in terms of 100% gas phase products.)

reactor with helium and then the deposited carbon was gasified in a hydrogen/helium 4 : 1 mixture at the same temperature and the effluent gas composition determined. The results of these experiments are presented in Table 3 which also contains for comparison purposes the composition of the gas generated from the decomposition of ethylene in the absence of a catalyst. Based on this data it is clear that in the case of copper–nickel there is a large fraction of methane which cannot be accounted for by hydrogasification of carbon. On the other hand, with a nickel catalyst it can be argued that within experimental error, the methane is formed entirely by the hydrogasification route.

2.5. Interaction of acetylene with copper–nickel and nickel. In a further series of experiments, the two catalysts were treated in the presence of acetylene in order to assess the influence of bond length in the hydrocarbon source on the reaction products. In these systems the partial pressure of acetylene was maintained at 100 Torr, the rest of the gas being helium or helium/hydrogen mixtures to overcome the effects of polymerization reactions which were found to occur at higher acetylene partial pressures. A comparison of the data obtained from the copper–nickel (3 : 7) and nickel-catalyzed decomposition of acetylene with that obtained using the same partial pressure of ethylene is given in Table 4. As expected, in both systems the decomposition of acetylene gave rise to higher amounts of carbon deposit than that derived from ethylene, but the gaseous product distribution was similar in each case.

2.6. Interaction of methane with copper–nickel and nickel. Finally, in order to determine the contribution of one of the major gaseous products, methane, toward the formation of carbon filaments, a series of experiments was performed in the flow reactor where methane to helium mixtures (1 : 3) were passed over copper–nickel (3 : 7) and nickel powders at temperatures ranging from 500 to 1000°C. From the data presented in Table 5, it can be seen that the onset of decomposition of methane in the absence of a catalyst occurs at 950°C and the presence of either copper–nickel or nickel does not appear to have any significant effect on the rate of this reaction. The observed reduction in the yield of both ethylene and acetylene at 1000°C when a metal is introduced into the system might be accounted for by the formation of solid carbon on the catalyst. It

TABLE 2

Percentage Carbon Distribution at 600°C as a Function of Ethylene/Hydrogen Ratio

$C_2H_4 : H_2$ Ratio	Hydrocarbon	Cu-Ni (3 : 7)	Ni
100 : 0	CH_4	19.8	0.9
	C_2H_4	1.3	93.8
	C_2H_6	4.6	1.6
	Solid carbon	74.3	—
4 : 1	CH_4	22.6	0.8
	C_2H_4	1.2	33.1
	C_2H_6	5.2	8.1
	Solid carbon	71.0	58.0
1 : 1	CH_4	24.9	1.0
	C_2H_4	4.7	41.3
	C_2H_6	12.5	13.5
	Solid carbon	57.9	44.2
1 : 4	CH_4	35.3	1.0
	C_2H_4	8.4	40.3
	C_2H_6	29.6	27.2
	Solid carbon	26.8	31.6

TABLE 3

Gas Product Analysis of Carbon Deposition followed by Hydrogasification on Copper–Nickel and Nickel Catalysts at 600°C

Gas analysis	Catalyst system				
	Cu : Ni		Ni		None
	Deposition[a]	Gasification[b]	Deposition[a]	Gasification[b]	Deposition[c]
CH_4	26.7	5.3	0.89	1.5	1.36
C_2H_4	0.76	—	16.6	—	92.7
C_2H_6	2.77	—	4.15	—	2.29
C_3 & C_4	0.33	—	0.13	—	3.69
H_2	69.7	73.6	78.3	78.2	—

[a] $C_2H_4 : H_2$ (80 : 20).
[b] $H_2 : He$ (80 : 20).
[c] C_2H_4 (100%).

is interesting to find that, under these conditions within experimental error, copper–nickel and nickel behave in an identical manner, suggesting that modifications of the surface of the bimetallic with respect to that which exists at lower temperatures might have occurred.

DISCUSSION

Formation of Filamentous Carbon from Catalyst Powders

It is apparent that the size of the initial metal powders used in the present study (~1 μm diam) have little bearing on the ultimate size of catalyst particles which are responsible for producing the carbon filament structures. The observation that the average width of filaments ranged from 25 to 100 nm suggests that prior to growth, fragmentation of the initial metal surface occurs. Break up of metal surfaces has been investigated in detail by Weisweiler and Mahadevan (*32*) who explained this phenomenon on the basis that when carbon was dissolved in the bulk metal, changes in the surface energy and wetting characteristics occurred which resulted in the formation of a system consisting of nucleated small particles containing dissolved carbon in contact with the metal surface. Catalyst particle fragmentation has been directly observed with controlled atmosphere electron microscopy when metal particles were heated in the presence of acetylene at 600°C (*33*). Other

TABLE 4

Comparison of Carbon Distribution from Ethylene and Acetylene over Copper–Nickel (3 : 7) and Nickel at 600°C

Product	Cu–Ni/C_2H_4	Cu–Ni/C_2H_2	Ni/C_2H_4–H_2	Ni/C_2H_2–H_2
CH_4	14.6	1.6	0.4	1.3
C_2H_2	—	8.2	—	20.4
C_2H_4	5.6	0.3	53.4	2.1
C_2H_6	3.9	0.05	5.5	0.4
Solid carbon	75.8	89.6	40.8	73.5

Note. Partial pressure of each hydrocarbon is 100 Torr.

TABLE 5

Decomposition of Methane/Helium (1 : 3) as a Function of Catalyst and Temperature (Carbon Distribution)

Catalyst	Temp. (°C)	CH_4	C_2H_4	C_2H_2	C_2H_6	% Solid carbon
None	900	99.8	0.1	—	0.05	—
	950	79.4	2.6	1.9	0.2	15.9
	1000	60.4	3.8	2.2	0.2	33.4
Cu–Ni	900	99.4	0.1	—	0.05	0.6
	950	77.8	1.7	1.3	0.1	19.1
	1000	57.1	2.8	1.0	0.1	39.0
Ni	900	99.7	0.1	—	0.05	0.1
	950	77.9	2.5	1.5	0.1	18.0
	1000	57.9	3.2	1.7	0.1	37.1

workers (*34*) have invoked this process to account for the formation of carbon filaments from metal foils.

Further evidence for the occurrence of fragmentation of metal particles is the pattern of growth characteristics presented in Fig. 3, which suggests that the carbon deposition reaction takes place in a sequential fashion. Initially, prolific filament growth takes place on the exposed metal surfaces which results in the removal of a small fraction of particles from the bed. As a consequence fresh catalyst particles located beneath the carbon layer become activated and this chain of events is repeated until all the catalyst is consumed.

Microscopic Features of the Catalyst Particles

Although the starting form of the catalyst was that of a powder, it is evident that during interaction with the hydrocarbon and the subsequent filament growth process, preferential orientation of the crystallites occurred. The crystallographic orientations generated at the metal–carbon and metal–gas interfaces have been identified by selected area electron diffraction (*35*). Other workers (*36–38*) have used LEED and Auger electron spectroscopy to identify the respective faces of nickel which dissolve and precipitate carbon. Based on these studies, it is clear that the orientation of the particle is a key factor in determining its ability not only to decompose a hydrocarbon molecule but also to initiate and sustain carbon filament growth.

A very unique bidirectional filament growth form is produced when nickel and certain nickel alloys are reacted in hydrocarbon environments (Fig. 1). It has been established by dark field imaging performed in the transmission electron microscope that in this type of filament structure the catalyst particle consists of a twinned crystal (*39*). Continuous observation of this growth process has shown that the filament limbs grow simultaneously from two opposite faces of the catalyst particle at identical rates (*40*). This feature indicates the existence of two uniform carbon diffusion pathways.

FLOW REACTOR STUDIES

Catalytic Activity in Ethylene

The present investigation has shown that there are major differences in the catalytic behavior of copper–nickel and nickel toward carbon deposition during interaction with ethylene. An important feature which has hitherto been neglected in the model of carbon filament formation is the restrictions imposed by the mode of interaction of the hydrocarbon with the metal surface. There is a considerable body of information which demonstrates that the various faces of nickel crystallites exhibit different abilities to adsorb and decompose hydrocarbons. It has been shown by several groups that the Ni(100) faces are particularly susceptible to build up of graphite overlayers (*41–43*), and it was also suggested that C–C bond activation is not a facile process on this face (*44*). Other workers have argued that filamentous carbon is produced when the hydrocarbon adsorbs and decomposes at the Ni(111) face (*45, 46*). It is tempting therefore to rationalize the findings in the current study according to the notion that in pure ethylene reaction takes place on faces that favor the formation of a graphite overlayer, which prevents further decomposition of hydrocarbon. Under these circumstances, the weight of carbon produced on the catalyst will be extremely low and possibly below the detection limits of the techniques used in the present work.

In contrast, when the bimetallic system is heated in pure ethylene, prolific carbon filament growth occurs (Fig. 4). The reasons for this difference in activity may lie in the manner by which ethylene adsorbs and subsequently reacts on the two catalyst surfaces. It would appear that copper–nickel is capable of breaking the carbon–carbon bound in the ethylene molecule and that under these circumstances polymerization reactions leading to surface graphite formation are averted. In this case, the carbon species formed on the surface dissolve in and diffuse through the catalyst and eventually precipitate to form the filament.

Based on the results of the current study it is clear that certain copper–nickel mixtures exhibit higher activity than nickel for both carbon deposition and hydrogasification of carbon. These findings are consistent with the data reported by Nishiyama and Tamai (*5, 6*) from the copper–nickel-catalyzed decomposition of benzene. These workers suggested that the enhanced activity of the bimetallic system was due to the creation of lattice defects in the metal crystallites. There is little doubt that such crystallographic imperfections would play an important role in promoting the growth of filamentous carbon since their presence will facilitate the diffusion of carbon through the catalyst particles.

Catalytic Activity in Ethylene–Hydrogen Mixtures

Examination of the data presented in Fig. 4 shows that the addition of hydrogen to the reactant stream produces some fascinating changes in the ability of both catalyst systems to produce solid carbon. It is probable that the progressive decrease in the weight of carbon produced on the copper–nickel (3 : 7) catalyst as hydrogen is added to the hydrocarbon feed is a result of catalytic hydrogasification of this material. This trend is not totally unexpected in view of the high catalytic activity of copper–nickel for the carbon–hydrogen reaction (*47*). In the case of nickel, the hydrogen additive appears to have a dual role promoting the formation of carbon up to a critical ratio (50% hydrogen in the carrier) and, at higher levels, acting in the same manner as that found with the bimetallic catalyst system. It is interesting to compare this latter dependence with that reported by Walker and coworkers [48] from their investigation of the influence of hydrogen on carbon formation from the disproportionation of carbon monoxide over an iron catalyst, where maximum amounts of carbon were formed when the gas mixture contained 40% hydrogen.

The promotional effect of hydrogen on carbon formation has been interpreted in two ways. Walker and co-workers (*48*) and Yang and Yang (*49*) suggested that the effect was related to the ability of hydrogen to decompose inactive metal carbides to the catalytically active metallic form. The other interpretation is that hydrogen removes the graphite overlayer which hinders the catalytic action of the metal (*6*). Adsorbed hydrogen may be performing the same function as copper, i.e., limiting the size of nickel ensembles, and thereby reducing the tendency for surface polymerization of ethylene to occur. A further possibility which must be taken into account is the ability of hydrogen to induce reconstruction of the nickel to produce a surface which favors carbon solubility rather than precipitation leading to the formation of the graphite overlayer. There is evidence from surface science studies that reconstruction of nickel surfaces occurs during adsorption of hydrogen (*50, 51*).

The inhibiting effect of hydrogen has also been reported (*6, 52, 53*) and claimed to be due to a decrease in the concentration of adsorbed carbon species resulting from surface hydrogenation reactions and also hydrogasification of carbon to form methane. A detailed kinetic study by Holstein and Boudart (*54*) has shown that in catalytic hydrogasification of graphite, the rate-determining step involves the rupture of carbon–carbon bonds by the catalyst leading to the formation of metal–carbon bonds, which subsequently react with adsorbed hydrogen to produce methane. From a combination of the thermogravimetric data shown in Fig. 5 and the gaseous product analysis, Fig. 6, it is evident that copper–nickel (3 : 7) is significantly more active than nickel for the hydrogasification of carbon to produce methane. This trend is particularly apparent in the temperature region, 550 to 700°C, and these conditions coincide with those where maximum yields of carbon are produced. A similar conclusion was reached by Baker and co-workers (*47*) who used *in situ* transmission electron microscopy to follow the behavior of these additives on the graphite–hydrogen reaction and also to determine the detailed kinetics from the action of individual catalyst particles.

Gas Phase Product Analysis

Perhaps some of the most useful information regarding the mechanism by which the hydrocarbon interacts with the metal surface can be obtained by careful interpretation of the gas product distribution. Methane is the major gaseous product from the interaction of ethylene/hydrogen with copper–nickel and might be expected to arise from hydrogasification of the carbon deposit. It is apparent that the amount of methane produced from this reaction is insufficient to account for the total methane yield produced during the carbon deposition reaction. Sequential carbon deposition/hydrogasification experiments have shown that the yield of methane from the copper–nickel/ethylene reaction is approximately five times the amount which results from hydrogasification of solid carbon. As a consequence, this product must arise from other reactions such as fragmentation of the adsorbed ethylene species. Examination of the corresponding data for a nickel catalyst undergoing the same reactions indicates that here all of the methane can be accounted for by hydrogasification of deposited carbon. This difference in the origin of methane would seem to imply that the nature of the adsorbed species on the bimetallic is quite different to that on pure nickel.

The finding that temperatures in excess of 900°C are required for uncatalyzed decomposition of methane are in accord with earlier studies (*55, 56*). It has been reported that when the reaction is performed over a nickel-containing catalyst, then the filamentous form of carbon can be produced at temperature as low as 500–650°C (*8, 57, 58*). Evans and co-workers (*59*) pointed out that the temperature at which solid carbon deposits were formed on nickel from interaction with methane were highly dependent on the purity of the gas; using a commercial grade source of methane they identified the presence of carbon deposits on nickel after reaction at 500°C, whereas with high purity methane carbon deposition did not occur until the temperature was increased above 900°C. The experiments reported here were carried out with high purity methane and demonstrate that the presence of either copper–nickel or nickel has very little effect on the rate of decomposition of methane and so we may conclude that under our conditions decomposition of methane does not contribute to any significant degree to the overall yield of solid carbon.

A further distinction in the nature of the gaseous products is the finding that the reaction of ethylene/hydrogen mixtures over nickel produces an amount of ethane based on the amount of ethylene converted significantly larger than that formed when the reaction is performed over copper–nickel (Table 2). This is further evidence of differences in the mode by which ethylene is adsorbed on these two metal surfaces. It is evident that the interaction of the olefin with nickel results in an intermediate which can readily undergo hydrogenation to form ethane, whereas the same reaction is not as favorable over copper–nickel.

The interactions of hydrocarbons with well-characterized metal surfaces have been extensively investigated by surface scientists because of their numerous implications in catalysis and related phenomena. The availability of high-sensitivity spectroscopic techniques has enabled researchers to identify the nature of some of the intermediate species formed at the surface of the metal. The pioneering efforts of Somorjai and his co-workers (*60*) led to the postulation of the existence of an ethylidyne intermediate from the adsorption of ethylene and acetylene on the Pt(111) surface. Initially an arrangement is formed where each carbon atom is bonded to a corresponding metal atom as depicted in Fig. 7a. On heating, this conformation is transformed into a new structure known as "ethylidyne" where one of the carbon atoms is attached to three metal atoms as illustrated in Fig. 7b. Recently, Zhu and White (*61*) reported on a detailed examination of the interaction of ethylene and acetylene on Ni(111) and concluded that for both hydrocarbons the likelihood of formation of ethylidyne was strongly dependent on the fraction of the surface coverage of the metal, this intermediate only being formed at near-saturation levels of these gases.

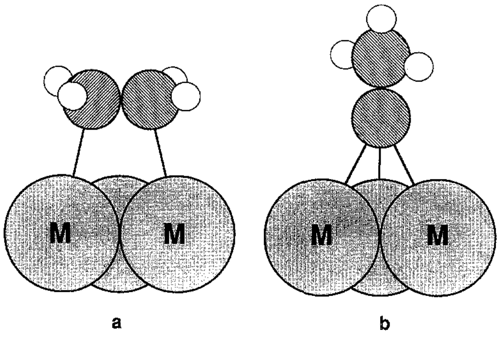

FIG. 7. Structural arrangement for (a) hydrocarbon bonded parallel to metal surface and (b) hydrocarbon bonded to metal in the stable "ethylidyne" conformation.

Although the existence of such structures has been established at temperatures well below those at which the current studies were performed, it should be possible to use the surface science information in order to understand the reaction pathways by which the hydrocarbons are adsorbed and decomposed at the metal surface. In the case of copper–nickel for example, the high yield of methane formed during reaction with ethylene, which cannot be accounted for solely on the basis of hydrogasification of solid carbon, could be attributed to the decomposition of the ethylidyne structure by rupture of the carbon–carbon bond generating methane and leaving behind a carbon deposit precursor on the metal surface. In contrast, the finding that when nickel interacts with ethylene lower amounts of methane are formed along with an appreciable yield of ethane would indicate that the adsorbed molecule does not rearrange to ethylidyne. Based on these arguments, examination of the product distributions obtained from acetylene leads to the conclusion that the ethylidyne intermediate was not formed on either copper–nickel or nickel at the conditions where current experiments were performed.

It should be appreciated that the existence of various structural arrangements of the hydrocarbon on the metal surface discussed above only provide a framework whereby the various gaseous products are formed, and does not furnish an understanding of the steps leading to carbon deposition which is dependent on the ability of the metal to break the carbon–carbon bond in the hydrocarbon. This state is achieved when the activation energy of the reaction with the metal surface is significantly larger than the heat of adsorption (*62*). It is possible that the presence of chemisorbed hydrogen can play a role in enhancing the strength of the metal–carbon bond and as a consequence a certain hydrogen level promotes carbon deposition on nickel (*63*).

CONCLUSIONS

1. This study has highlighted an aspect of catalytic carbon deposition which has hitherto been ignored, namely the importance of the nature of the interaction of the carbon-containing gas with the metal surface. One cannot assume a priori that because a hydrocarbon is adsorbed on the metal surface, fragmentation of the molecule leading to carbon deposition will necessarily occur. Such a step requires the formation of a relatively strong metal–carbon bond and the concomitant rupture of a carbon–carbon bond in the hydrocarbon molecule. In addition, it is also apparent that the distribution of the gas phase products arising from such an interaction is directly related to the structural conformation of the most favored hydrocarbon arrangement adsorbed at the metal surface. Based on these arguments, it is now possible to understand the inability of methane to readily undergo interaction with metals to produce carbon deposits at temperatures below 900°C.

2. A further aspect to emerge from this investigation is the finding of an intimate link between the role of a metal catalyst in carbon deposition and in hydrogasification of carbon. In both cases the primary step involves the rupture of a carbon–carbon bond to form a carbon–metal bond. In the carbon deposition reaction, this phenomenon takes place between a carbon-containing gas and the metal, whereas in hydrogasification, the components are solid carbon and the metal. Previous studies (*64, 65*) have demonstrated the interplay between these two processes and how they can be reversed by careful manipulation of the hydrocarbon/hydrogen ratio.

3. The role of hydrogen in promoting the formation of solid carbon on nickel during interaction with ethylene is still not clearly understood. It is possible that adsorbed hydrogen may be inhibiting the polymerization of adsorbed ethylene molecules on the metal surface and as a consequence it may be performing the same function as copper, i.e., limiting the size of nickel ensembles and thereby reducing the potential for eventual deactivation by the formation of a graphite overlayer.

ACKNOWLEDGMENT

This work was supported by the National Science Foundation under Grant CBT-8800931.

REFERENCES

1. Baker, R. T. K., and Harris, P. S., *in* "Chemistry and Physics of Carbon" (P. L. Walker, Jr. and P. A. Thrower, Eds.), Vol. 14, p. 83. Dekker, New York, 1978.
2. Rostrup-Nielsen, J. R., "Steam Reforming Catalysts." Tekorisk Forlay A/S (Danish Technical Press), Copenhagen, 1975.
3. Bartholomew, C. H., *Catal. Rev.-Sci. Eng.* **24,** 67 (1982).
4. Trimm, D. L., *Catal. Rev.-Sci. Eng.* **16,** 155 (1977).
5. Nishiyama, Y., and Tamai, Y., *J. Catal.* **33,** 98 (1974).
6. Nishiyama, Y., and Tamai, Y., *J. Catal.* **45,** 1 (1976).
7. Vanstiphout, P. C. M., Stobbe, D. E., Scheur, F. Th. V. D., and Geus, J. W., *Appl. Catal.* **40,** 219 (1988).
8. Bernardo, C. A., Alstrup, I., and Rostrup-Nielsen, J. R., *J. Catal.* **96,** 517 (1985).
9. Tavares, M. T., Bernardo, C. A., Alstrup, I., and Rostrup-Nielsen, J. R., *J. Catal.* **100,** 545 (1986).
10. Best, R. J., and Russell, W. W., *J. Am. Chem. Soc.* **76,** 838 (1954).

11. Hall, W. K., and Emmett, P. H., *J. Phys. Chem.* **62,** 816 (1958).

12. Gharpurey, M. K., and Emmett, P. H., *J. Phys. Chem.* **65,** 1182 (1961).

13. Yamashina, T., and Farnsworth, H. E., *Ind. Eng. Chem. Prod. Res. Dev.* **2,** 34 (1963).

14. Van der Plank, P., and Sachtler, W. M. H., *J. Catal.* **12,** 35 (1968).

15. Sinfelt, J. H., Carter, J. L., and Yates, D. J. C., *J. Catal.* **24,** 283 (1972).

16. Ponec, V., and Sachtler, W. M. H., *J. Catal.* **28,** 376 (1973).

17. Beelen, J. M., Ponec, V., and Sachtler, W. M. H., *J. Catal.* **28,** 376 (1973).

18. Takasu, Y., and Shimizu, H., *J. Catal.* **29,** 479 (1973).

19. Dalmon, J. A., and Martin, G. A., *J. Catal.* **66,** 214 (1980).

20. Martin, G. A., and Dalmon, J. A., *J. Catal.* **75,** 233 (1982).

21. Dowden, D. A., and Reynolds, P., *Discuss. Faraday Soc.* **8,** 184 (1950).

22. Dowden, D. A., *J. Chem. Soc.,* 242 (1950).

23. Wynblott, P., and Ku, R. C., *Surf. Sci.* **65,** 511 (1977).

24. Helms, C. R., *J. Catal.* **36,** 114 (1965).

25. Ponec, V., Surf. Sci. **80,** 352 (1979).

26. Ponec, V., *in* "Advances in Catalysis" (D. D. Eley, H. Pines, and P. B. Weisz, Eds.), Vol. 32, p. 149. Academic Press, San Diego, 1983.

27. Sinfelt, J. H., "Bimetallic Catalysts," an Exxon Monograph. Wiley, New York, 1983.

28. Ponec, V., *Catal. Rev.-Sci. Eng.* **11,** 41 (1975).

29. Ertl, G., and Kuppers, J., "Low Energy Electrons and Surface Chemistry." Verlag Chemie, Weinheim, 1974.

30. Ohtani, H., Kao, C.-T., Van Hove, M. A., and Somorjai, G. A., *Prog. Surf. Sci.* **23,** 155 (1986).

31. Rohsenow, W. M., and Hartnett, J. P., "Handbook of Heat Transfer," pp. 2–83. McGraw-Hill, New York, 1973.

32. Weisweiler, W., and Mahadevan, V., *High Temp.-High Pressures* **4,** 27 (1972).

33. Baker, R. T. K., and Chludzinski, J. J., *J. Catal.* **64,** 464 (1980).

34. Sacco, A., Thacker, P., Chang, T. N., and Chiang, A. T. S., *J. Catal.* **85,** 224 (1984).

35. Yang, R. T., and Chen, J. P., *J. Catal.* **115,** 52 (1989).

36. Schouten, F. C., Kaleveld, E. W., and Bootsma, G. A., *Surf. Sci.* **63,** 460 (1977).

37. Schouten, F. C., Gijzeman, O. L. J., and Bootsma, G. A., *Surf. Sci.* **87,** 1 (1979).

38. Eizenberg, M., and Blakely, J. M., *J. Chem. Phys.* **71,** 3467 (1979).

39. Audier, M., Guinot, J., Coulon, M., and Bonnetain, L., *Carbon* **19,** 99 (1981).

40. Baker, R. T. K., Harris, P. S., and Terry, S., *Nature* **253,** 37 (1975).

41. McCarty, J. G., and Wise, H., *J. Catal.* **57,** 406 (1979).

42. Goodman, D. W., Kelley, R. D., Madey, T. E., and White, J. M., *J. Catal.* **64,** 479 (1980).

43. Nakamura, J., Hirano, H., Xie, M., Matsuo, I., Yamada, T., and Tanaka, K., *Surf. Sci.* **222,** L809 (1989).

44. Schoofs, G. R., and Benziger, J. B., *Langmuir* **4,** 526 (1988).

45. Leidheiser, H., and Gwathmey, A. T., *J. Am. Chem. Soc.* **70,** 1206 (1948).

46. Grenga, H. E., and Lawless, K. R., *J. Appl. Phys.* **43,** 1508 (1974).

47. Baker, R. T. K., Chludzinski, J. J., Bernardo, C. A., and Figueiredo J. L., *in* "Proceedings, 9th International Congress on Catalysis, Calgary, 1988" (M. J. Phillips and M. Ternan, Eds.), Vol. 3, p. 1059. Chem. Institute of Canada, Ottawa, 1988.

48. Walker, P. L. Jr., Raksawski, J. F., and Imperial, G. R., *J. Phys. Chem.* **63,** 140 (1959).

49. Yang, K. L., and Yang, T. T., *Carbon* **24,** 687 (1986).

50. Kleinle, G., Scottkie, M., Penka, V., Ertl, G., Behm, R. J., and Moritz, W., *Surf. Sci.* **189,** 177 (1987).

51. Voigtlander, B., Lehwald, S., and Ibach, H., *Surf. Sci.* **208,** 113 (1989).

52. Tottrup, R. B., *J. Catal.* **42,** 29 (1976).

53. Gardner, D. C., and Bartholomew, C. H., *Ind. Eng. Chem. Prod. Res. Dev.* **20,** 70 (1981).

54. Holstein, W. L., and Boudart, M., *J. Catal.* **72,** 328 (1981).

55. Eizenberg, B., and Bliss, H., *Chem. Eng. Prog., Symp. Ser.* **63**(72), 3 (1967).

56. Palmer, H. B., Lahaye, J., and Hou, K. C., *J. Phys. Chem.* **72,** 348 (1968).

57. Robertson, S. D., *Carbon* **10,** 221 (1972).

58. Rostrup-Nielsen, J. R., *J. Catal.* **27,** 343 (1972).

59. Evans, E. L., Thomas, J. M., Thrower, P. A., and Walker, P. L., *Carbon* **11,** 441 (1973).

60. Koestner, R. J., Frost, J. C., Stair, P. C., Van Hove, M. A., and Somorjai, G. A., *Surf. Sci.* **116,** 85 (1982).

61. Zhu, X. Y., and White, J. M., *Surf. Sci.* **214,** 240 (1989).

62. Kesmodel, L. L., Dubois, L. H., and Somorjai, G. A., *J. Chem. Phys.* **70,** 2180 (1979).

63. Dry, M. E., Shingles, T., Boschoff, L. J., and Van H. Botha, C. S., *J. Catal.* **17,** 347 (1970).

64. Baker, R. T. K., and Sherwood, R. D., *J. Catal.* **95,** 101 (1985).

65. Figueiredo, J. L., Bernardo, C. A., Chludzinski, J. J., and Baker, R. T. K., *J. Catal.* **110,** 127 (1988).